Finite element modelling of orthogonal cutting: sensitivity analysis of material and contact parameters

Michel Watremez, Damien Méresse, Laurent Dubar, Julien Brocail

Finite element modelling of orthogonal cutting: sensitivity analysis of material and contact parameters

Michel WATREMEZ, Damien MERESSE, Laurent DUBAR, Julien BROCAIL

Abstract

This paper presents a two-dimensional finite element model of orthogonal cutting. The proposed model is developed with Abaqus/explicit software. An Arbitrary Lagrangian-Eulerian (ALE) formulation is used to predict chip formation, temperature, chip-tool contact length, chip thickness, and cutting forces. This numerical model of orthogonal cutting is then validated by comparing these process variables to experimental and numerical results obtained by Filice et al. (2006). This model makes possible qualitative analysis of input parameters related to cutting process and frictional models. A sensitivity analysis is performed on the main input parameters (coefficients of the Johnson-Cook law, contact and thermal parameters) with the finite element model. This analysis allows the identification of significant parameters and their tolerance limits identification. This study draws to input parameters which have to be determined accurately as far as possible in order to improve numerical approaches of machining.

Keywords: Orthogonal cutting, finite element model, sensitivity analysis

1. Introduction

High speed machining is submitted to economical and ecological constraints. Optimization of cutting processes must increase productivity, reduce tool wear and control residual stresses in the workpiece. Developments of numerical approaches to simulate accurately high speed machining process are therefore necessary since in situ optimisation is long and costly. To get this purpose, rheological behaviour of both antagonists and representative friction model at tool chip interface have to be studied at very intense plastic strains (from 1 to 5), high strain rates (until 10^5 s^{-1}), and high temperature (until 1200 °C) as encountered during high speed machining process. These mechanical conditions have been mentioned in the works of first Özel and Altan (2000) while temperature distribution in cutting process are described by Outeiro et al. (2004).

The flow stress of the workpiece is usually described by the Johnson-Cook model. The Johnson-Cook parameters are usually obtained by split Hopkinson pressure bar but this testing device cannot unfortunately provide either high strain rates or high temperatures.

A set of different friction testing stand can be used to identify the friction parameters at the tool–chip interface. Device based on the pin-on-disc system has been first developed by Olsson et al (1989) but contact conditions of the machining process cannot be simulated by it. Contact pressure and temperature value of about 750 MPa and 950 °C, respectively, can be reached with the test proposed by Meiller et al. (2000). Friction devices, recently designed by Bonnet et al. (2008) and by Brocail et al. (2008), can reach relevant contact conditions in pressure and temperature. Very recent works led by Rech et al. (2009) suggest a friction model depending on the average sliding velocity. Brocail et al. (2008) have also proposed a new frictional model depending on sliding velocity and interfacial pressure and temperature. These both authors agree that using a coulomb model with constant friction coefficient is unsuitable to simulate friction phenomena at the tool-chip interface.

The both rheological and frictional behaviours influence the process variables such as the shape of deformation zones, temperatures and stresses distributions, contact length, chip thickness, and cutting forces. Many studies have showed the influence of input parameters such as the coefficients of the Johnson-Cook law reported by Umbrello et al. (2007) and the friction models studied by Özel (2006) and Brocail et al. (2010) on the process variables. The works of Haglund et al. (2008) deal with the impact of a set of parameters by studying the model sensitivity regarding each parameter.

The proposed two-dimensional finite element model of orthogonal cutting model is developed with Abaqus/explicit software and an Arbitrary Lagrangian-Eulerian (ALE) formulation is used to predict chip formation, temperature, chip-tool contact length, chip thickness, and cutting forces. A sensitivity analysis is conducted on the main input parameters with this finite element model. This study is divided into 3 parts and is performed with two levels for each factor in order to highlight the impact of one parameter. In the first part, the rheological parameters of the Johnson-Cook law are

studied. A second study is carried out on contact parameters such as thermal conductance K, heat partition coefficient α and Coulomb's coefficient μ. Finally, thermal parameters such as conductivity and specific heat are the subject of a third part.

2. Finite element model for orthogonal cutting analysis

In the present paper, two-dimensional cutting commonly known as orthogonal cutting is considered. A two-dimensional finite element model for orthogonal cutting is implemented with a commercial software code, ABAQUS and explicit dynamic ALE formulation is chosen to avoid computation problems.

2.1. Description

Initial workpiece and tool mesh configuration is illustrated by Fig.1. The chip-formation zone is only meshed. Four node bilinear displacement and temperature quadrilateral elements CPE4RT are used for both workpiece and tool in order to enable coupled temperature-displacement calculations.

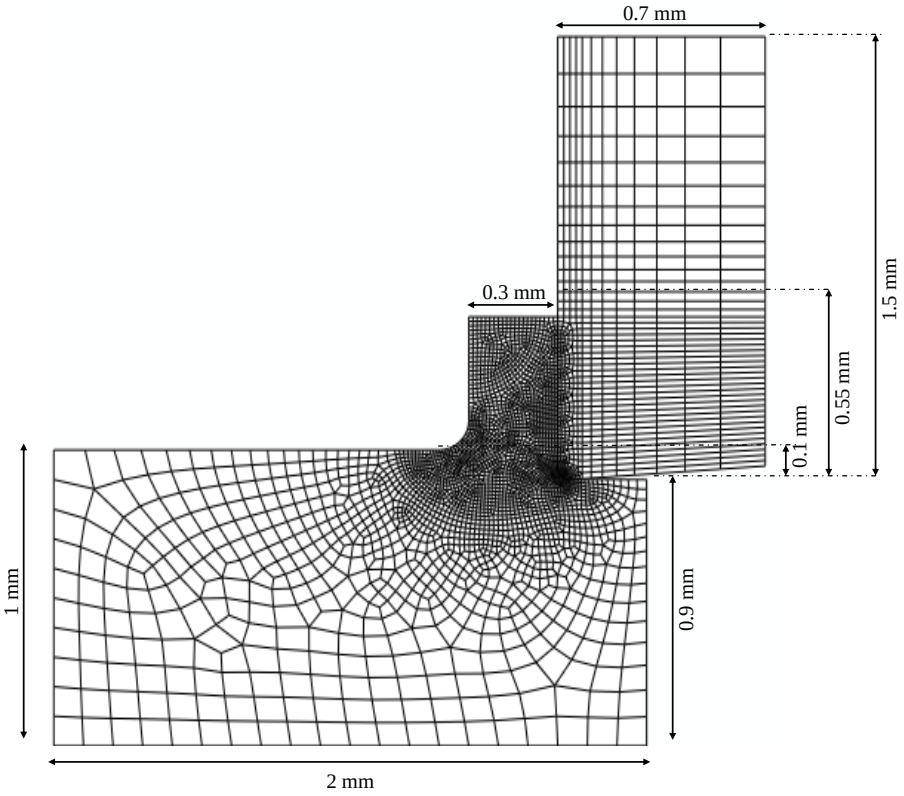

Fig. 1. Initial mesh configuration of numerical model.

A refined mesh is necessary in the high deformation zones (primary shear zone and secondary shear zone) and in the zone near the cutting edge. In the case of 0.1 mm feed, elements located in the high deformation zones and in the

contact zone have a 10 μm size. Smaller elements of 5 μm size are located in the tool tip. Apart from these zones, elements dimensions vary from 10 μm to 100 μm. 2850 elements and 700 elements are respectively used for the finite element mesh of the workpiece and the tool.

During machining processes, an amount of heat is induced by plastic deformation of the workpiece in the primary and secondary shear zone and by friction at the tool-chip interface. The mechanical energy due to plastic deformations is converted into heat by the ratio of Taylor-Quinney coefficient. The heat equation involving the plastic deformations, the heat and the Taylor-Quinney coefficient can be expressed as:

$$\beta.\sigma_m.\frac{\partial \varepsilon_{pl}}{\partial t} = \rho.c_p.\frac{\partial T}{\partial t} \quad (1)$$

with β Taylor-Quinney's coefficient, σ_m mean stress, ε_{pl} plastic strain, ρ density, c_p specific heat and T temperature. In agreement with the works of Rosakis et al. (2000), the coefficient of Taylor-Quinney is set equal to 0.9. The heat flux generated by friction depends on shear stress, sliding velocity and ratio of friction energy converted into heat:

$$\varphi = \eta.\tau.\frac{\partial x}{\partial t} \quad (2)$$

Here φ is heat flow rate generated by friction, η is ratio of friction energy converted into heat, τ is shear stress and x corresponding to displacement. In this work, the ratio η is set equal to 100 %. The heat flux due to friction phenomena is divided between specimen and contactor in accordance with their thermal effusivities and 60 % of the heat flow rate generated is affected to the specimen.

The interfacial behaviour between contactor and specimen is modelled by a Coulomb's friction model. The friction coefficient introduced in the model is set constant for the interface between the contactor and the specimen.

Displacement and thermal boundary conditions applied to the workpiece and tool are shown by Fig. 2. The workpiece is modelled with Eulerian surfaces at both left and right boundaries and at the top surface of the chip whereas lagrangian boundaries are used at the top and the bottom of the workpiece. Material enters the workpiece on the "in flow" surface with a temperature of 20 °C and exits the workpiece at both out flow and chip flow surface. By default, the mesh is not fixed spatially on these boundaries. The surface mesh should be fixed in space using special mesh constraints. Mesh constraints must be applied to prevent the mesh from moving with material. These constraints applied normal to Eulerian boundaries allow material to flow into or out of the mesh. In order to stop the barrel effect, constraints are applied tangential to "in flow" surface. The material flowing into Eulerian boundary is assumed to have the same properties as the workpiece material. The cutting speed V_c is applied to the inflow boundary of the workpiece. The workpiece is fixed at the bottom and the tool is totally fixed as represented in Fig. 2. The tool has a 50 micrometer edge radius and is modelled as rigid body with thermal conductivity.

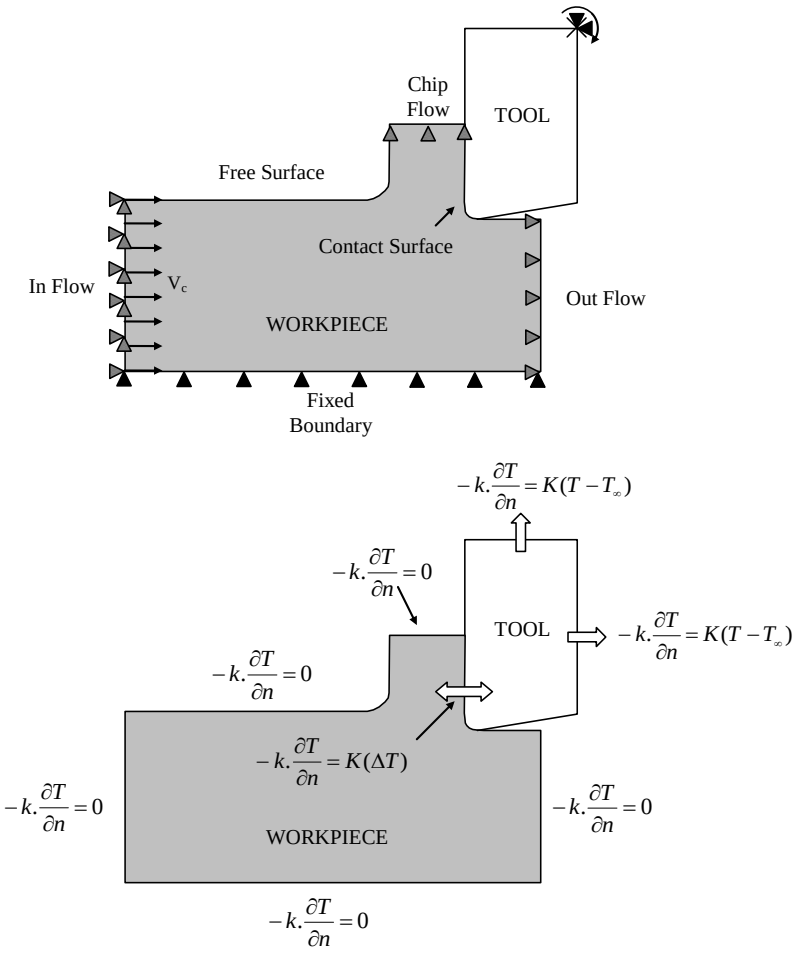

Fig. 2. Displacement and thermal boundary conditions.

For thermal boundary conditions, workpiece and tool are initially set at 20 °C. The chip-tool contact is assumed as thermally perfect for the heat transfer computing by taking into account a high thermal conductance (10^6 °C.w^{-1}.m^{-2}). In order to obtain relevant interfacial temperature, the model includes the heat generation induced by plastic deformation and by friction. Workpiece boundaries far away from the contact zone are dealt without any heat loss either by convection or by radiation. These heat losses are very small and negligible such as claimed by Yen et al. (2004). In order to prevent the heat accumulation, conduction is applied by means of an analytic rigid surface placed on external boundaries of tool. A very low thermal contact resistance allows evacuating heat from the tool.

The ALE model requires pre-defined chip geometry. During the simulation of cutting process, the chip thickness and the chip-tool contact length gradually change to their final size. The chip formation progress during the orthogonal cutting simulation is shown on Fig.3 for a machining time of 12 ms. The geometry and forces are almost stabilized after 1.6 ms. Longer time is needed to reach a steady state for the temperature distribution at the chip-tool interface.

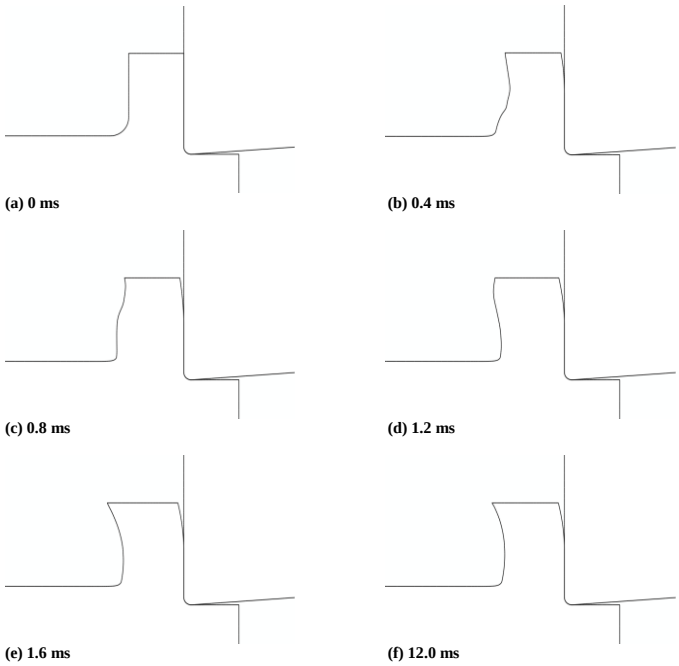

Fig. 3. Progress of chip formation during an orthogonal cutting simulation.

The major drawback of this approach is the necessity of pre-define the chip. Adjustment difficulties appear in the meshing as shown in Fig. 4. The chip flow is kept in vertical position and therefore, this Eulerian surface can not adjust itself to be normal to the chip radius. Thus, the initial chip thickness is an estimation of the expected chip shape in steady state.

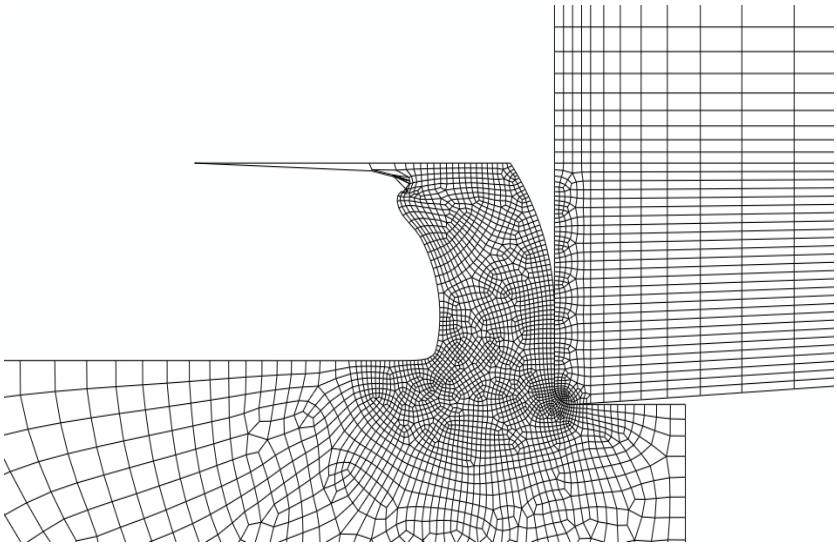

Fig. 4. Adaptive meshing error.

2.2. Validation

This orthogonal cutting model is validated by comparing some process variables to experimental and numerical results obtained by Filice et al. (2006). Their experimental tests have been performed without lubrificant, with a cutting

speed of 100 m.min^{-1}, a feed of 0.1 mm and a depth of cut of 3 mm. Workpiece and tool materials are respectively AISI 1045 steel and uncoated carbide, with a rake angle of 0° and a clearance angle of 4°. Their experimental conditions are summarized in table 1.

Table 1. Experimental conditions.

Workpiece material	AISI 1045
Tool material	Uncoated carbide
Cutting speed (m.min^{-1})	100
Feed (mm)	0.1
Depth of cut (mm)	3
Rake angle (°)	0
Clearance angle (°)	4

Five friction models have been implemented in their finite element model of machining. For each friction model, optimum friction factors are obtained by optimisation. This study shows that numerical approaches using these current friction models do not generate good correlations of process variables, such as cutting force and most of all thrust force and tool-chip contact length. More similar differences are also found with other friction models. Best numerical results are obtained with a Coulomb's friction coefficient equal to 0.4 and are given by table 2.

Table 2. Experimental and numerical results obtained by Filice et al. (2006).

	Experimental	Numerical (μ=0.4)
Cutting force (N)	745	761
Thrust force (N)	600	430
Contact length (mm)	0.5	0.26
Chip thickness (mm)	0.29	0.20
Shear angle (deg)	19	27
Measured temperature (°C)	542	555

Results of our suggested model have to be compared with best numerical and experimental results obtained by Filice et al. (2006). The workpiece material (AISI 1045 steel) is modelled as a thermo-viscoplastic material. A Johnson-Cook model represented as equation 3 describes the flow stress of AISI 1045 steel according to strain, strain rate and temperature:

$$\sigma = \left[A + B \cdot \varepsilon_{pl}\right]^{n} \cdot \left[1 + C \cdot \ln\left(\frac{\dot{\varepsilon}_{pl}}{\dot{\varepsilon}_{0}}\right)\right] \cdot \left[1 - \left(\frac{T - T_{room}}{T_{melt} - T_{room}}\right)^{m}\right] \quad (3)$$

with σ flow stress, A yield strength, B hardening modulus, ε_{pl} plastic strain, n hardening coefficient, C strain rate sensitivity coefficient, $\dot{\varepsilon}_{pl}$ plastic strain rate, $\dot{\varepsilon}_0$ reference plastic strain rate, T temperature of the workpiece, T_{room} room temperature, T_{melt} melting temperature of the workpiece, and m thermal softening coefficient.

The Johnson-Cook parameters come from works of Jaspers et al. (2002) and are reported in table 3. The material flow characteristics are obtained by split Hopkinson pressure bar but this test cannot unfortunately provide both high strain rates and high temperatures.

Table 3. Johnson-Cook's parameters from Jaspers et al. (2002)

A (MPa)	B (MPa)	n	C	m	$\dot{\varepsilon}_0$ (s-1)	T_{melt} (°C)	T_{room} (°C)
553.1	600.8	0.234	0.0134	1	1	1460	20

The Johnson-Cook parameters are presumed to be reliable for cutting conditions as mentioned by Jovic et al. (2006). The thermo-physical properties of the specimen have been considered from works of Grzesik (2004) and are summed up in table 4. The thermo-physical properties of uncoated carbide H13A tool are chosen in accordance with Kalhori's works (2001) and the selected data are reported in table 5.

The interaction between workpiece and tool is defined by applying a contact model based on Coulomb's friction law. The friction coefficient introduced in the model is set constant to 0.4. The process variables (such as the cutting force, the thrust force, the chip thickness, and the contact length) predicted by this model for reference conditions described by Table 1 are compared with variables got experimentally and numerically by Filice et al. (2006). The cutting force predicted by this numerical model is greater than the experimental cutting force obtained by Filice et al. (2006) as suggested by Fig. 5. The predicted feed force is significantly lower than the experimental reference (relative error of 30%). The value of 0.31 mm obtained in Abaqus for the chip thickness is perceptibly equal to experimental value. Comparing the predicted process variables with the experimental values, significant errors are observed for the feed force and the contact length. Nevertheless, results got with the orthogonal cutting model are perceptibly equal to numerical results obtained by Filice et al. (2006). This numerical model of orthogonal cutting can be considered to be reliable enough to make qualitative analysis of input parameters related to cutting process and frictional models.

Table 4. Thermo-physical properties of the AISI 1045 workmaterial from Grzesik (2004)

Parameter	Temperature (°C)	Value
Elasticity (E) ($N.m^{-2}$)	20	2.15×10^{11}
	200	2.10×10^{11}
	400	1.65×10^{11}
	600	1.60×10^{11}
	800	0.90×10^{11}
Density (ρ) ($kg.m^{-3}$)	20	7800
	200	7740
	400	7665
	600	7595
	800	7585
	1000	7520
Thermal conductivity ($W.m^{-1}.°C^{-1}$)	25	45.1
	125	42.7
	325	37.9
	525	33.2
	725	28.4
	925	24.9
	1125	27.0
Specific heat (c_p) ($J.kg^{-1}°C^{-1}$)	25	435.3
	125	488.3
	325	559.0
	525	686.1
	725	1171.0
	925	808.2
	1125	789.1
Expansion	100	11×10^{-6}
	200	12×10^{-6}
	300	13×10^{-6}
	400	14×10^{-6}
	500	14×10^{-6}
	600	15×10^{-6}
	700	15×10^{-6}

Table 5. Thermo-physical properties for the carbide substrate.

Parameter	Value
Elasticity (E) ($N.m^{-2}$)	Rigid
Density (ρ) ($kg.m^{-3}$)	14500
Thermal conductivity ($W.m^{-1}.°C^{-1}$)	25.0
Specific heat (c_p) ($J.kg^{-1}°C^{-1}$)	220.0

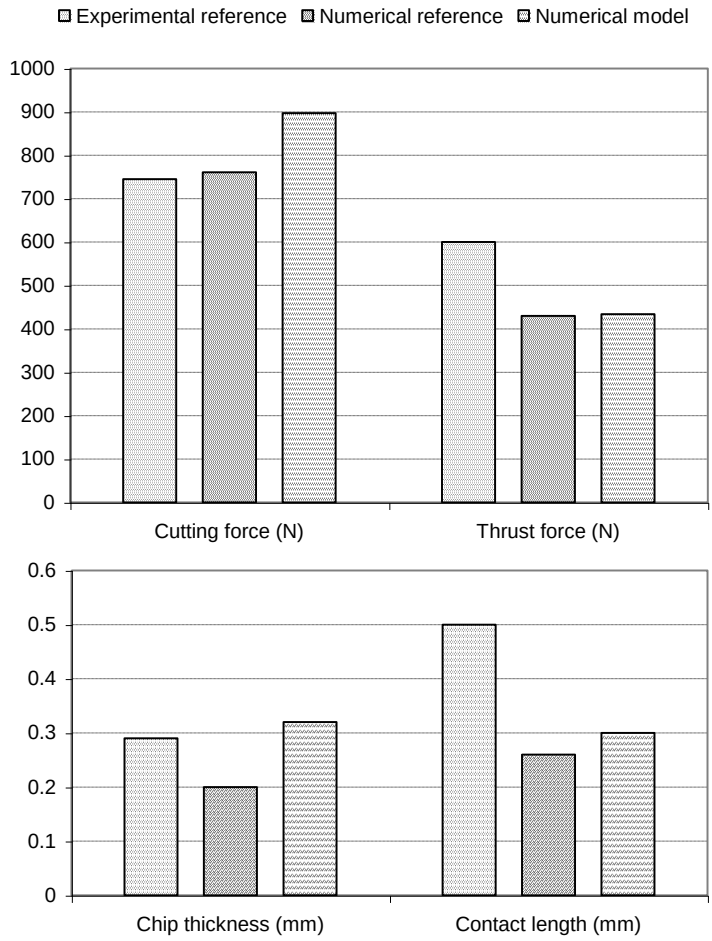

Fig. 5. Predicted process variables for the reference conditions.

3. Sensitivity analysis of finite element model.

The impact of main input parameters reported in Table 6 and the accuracy of their values are considered for the sensitivity analysis. For this study, a full factorial experiment can not be envisaged, even if each factor has only two levels. With twelve factors each taking two levels, a factorial experiment would have 4096 treatment combinations. This study is divided into 3 parts. The first part is about the rheological parameters of the Johnson-Cook law and a second study is subsequently carried out on the contact parameters. The sensitivity of thermal parameters is the subject of a third party.

Table 6. Reference parameter values for sensitivity analysis from Jaspers et al (2002) and Grzesik (2004)

Parameters		Reference values
Johnson-Cook law	A (MPa)	553.1
	B (MPa)	600.8
	C	0.0134
	m	1
	n	0.234
Contact	Thermal conductance K ($W.m^{-2}.°C^{-1}$)	10^6
	Heat partition coefficient α	0.6
	Friction coefficient μ	0.4
Thermal	Workpiece conductivity ($W.m^{-1}.°C^{-1}$)	45.1 (25 °C) 42.7 (125 °C) 37.9 (325 °C) 33.2 (525 °C) 28.4 (725°C) 27.0 (775°C) 25.4 (825 °C) 24.9 (875°C) 24.9 (925 °C) 25.4 (975°C) 26.0 (1025 °C) 26.5 (1075°C) 27.0 (1125°C)
	Workpiece specific heat ($J.kg^{-1}.°C^{-1}$)	435.1 (25 °C) 488.3 (125 °C) 559.0 (325 °C) 686. 1(525 °C) 1171.0 (725 °C) 1077.6 (775 °C) 993.1 (825 °C) 906.8 (875 °C) 808.2 (925 °C) 778.3 (975 °C) 781.9 (1025 °C) 785. 5 (1075 °C) 789.1 (1125 °C)
	Tool conductivity ($W.m^{-1}.°C^{-1}$)	25
	Tool specific heat ($J.kg^{-1}.°C^{-1}$)	220

3.1. Impact of rheological parameters

The impact of rheological parameters on process variables are analysed with the Johnson-Cook law. The numerical model has been validated with Johnson-Cook parameters given by Jaspers et al. (2002). Ôzel and karpat (2007) have also determined parameters of the Johnson-Cook law for an AISI 1045 steel. Meyer et al. (2006) have obtained other values. Table 7 shows all these parameters found in the literature for an AISI 1045 steel. These laws have to be implemented in the finite element model of orthogonal cutting. Johnson-Cook parameters affect the values of predicted process variables as shown in Table 8. The chip thickness e varies of 30 % maximum, while the contact length l_c ranges from 0.29 mm to 0.35 mm, ie a difference of 20 %. The temperature difference for the chip $T_{c\ max}$ and tool $T_{o\ max}$ is less than 10 %. A large range of variation is observed for the cutting forces (30 % for the cutting force F_c and 22 % for thrust force F_t).

Table 7. Johnson-Cook parameters for an AISI 1045 steel.

	***A* (MPa)**	***B* (MPa)**	***C***	***m***	***n***
Jaspers (Ref.)	553.1	600.8	0.0134	1	0.234
Ozel[1]	451.6	819.5	0.0000009	1.0955	0.1736
Ozel[2]	646.19	517.7	0.0102	0.94054	0.24597
Ozel[3]	731.63	518.7	0.00571	0.94054	0.3241
Ozel[4]	546.83	609.35	0.01376	0.94053	0.2127
Meyer	-20.6	1226.5	0.017	1.005	0.193

Table 8. Predicted process variables for Johnson-Cook laws.

	$T_{o\ max}$ (°C)	**$T_{c\ max}$ (°C)**	**l_c (mm)**	**e (mm)**	**F_c (N)**	**F_t (N)**
Jaspers (Ref.)	635	636	0.30	0.32	897	434
Ozel[1]	657	659	0.34	0.38	982	456
Ozel[2]	611	611	0.29	0.31	847	415
Ozel[3]	647	647	0.33	0.36	955	449
Ozel[4]	619	617	0.29	0.30	849	420
Meyer	712	711	0.35	0.37	1109	508

To discern the impact of one parameter, a sensitivity analysis is performed with two levels for each factor as reported in Table 9. These values are chosen in accordance with works of previously named authors. Johnson-Cook parameters proposed by Meyer et al. (2006) generate an excessive meshing distortion. So, these coefficients are not considered.

Table 9. Level values for Johnson-Cook law.

	Low level	**High level**
A (MPa)	451.6	731.63
B (MPa)	517.7	819.5
C	0.0000009	0.01376
m	0.94053	1.0955
n	0.1736	0.3241

The impact of Johnson-Cook parameters on temperatures results is represented in Fig. 6. The increase of all coefficients generates greater values of maximum temperature, while the interactions are insignificant. A rising temperature of 11% is observed when the value of hardening modulus is increased. Rising temperature generated by the

other coefficients ranges from 3 to 6 %. The increase of coefficients leads to increase the flow stress. So, the workpiece material is harder, and machining generates more important temperatures.

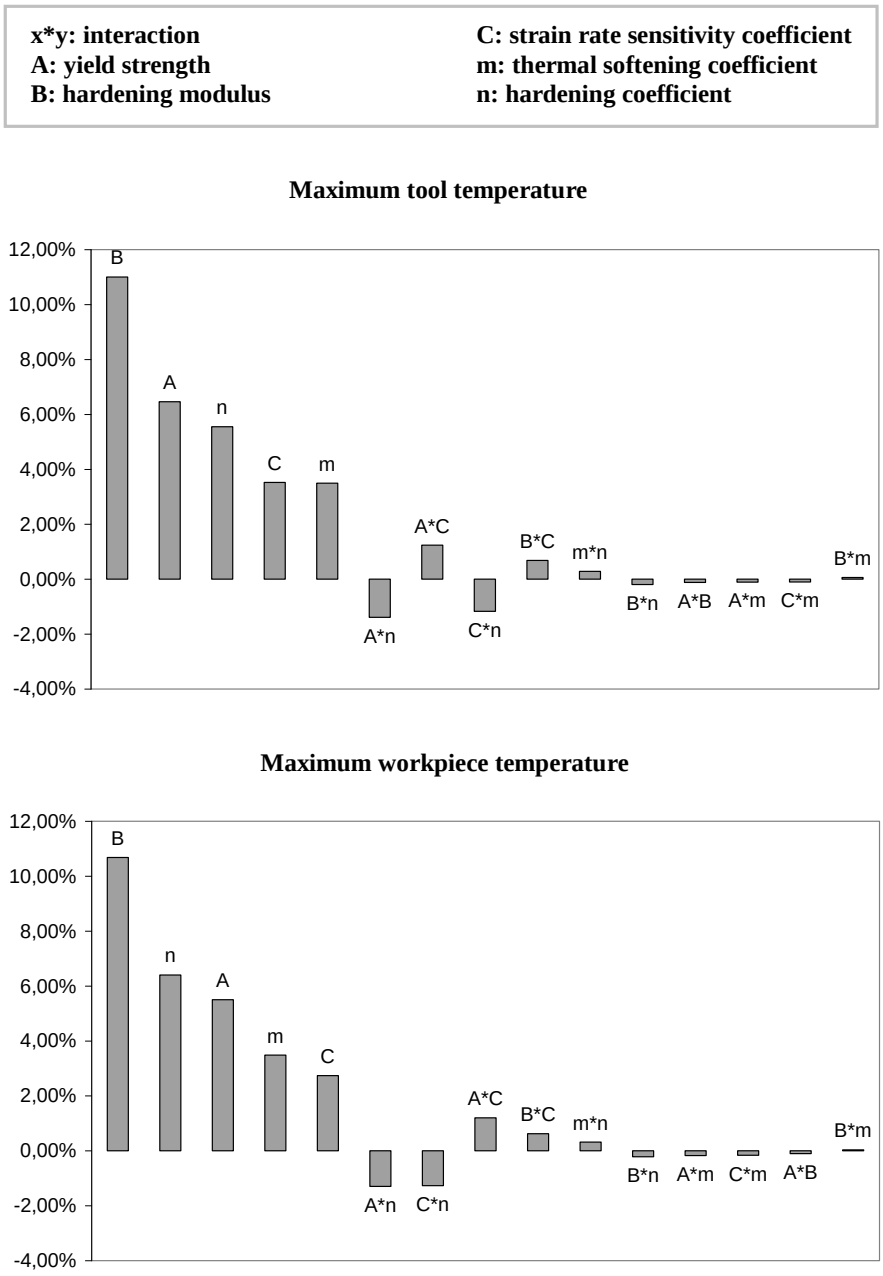

Fig. 6. Impact of Johnson-Cook parameters on the maximum temperatures.

The contact length and the chip thickness are affected by coefficients n, A, and C, while interactions and other coefficients have insignificant effects on these predicted variables as shown in Fig.7. The increase of hardening coefficient n leads to lengthening of surface contact (+ 28 %) and a chip thicker (+32 %). Contact length decreases respectively of 20 % and 17 % when the coefficients A and C increase, while chip thickness decreases of 25 %.

The change from low level to high level of parameters n, B, and m generates a rising of the cutting force as suggested in Fig. 8. The greatest factor is the hardening coefficient n with an effect of 28 %, followed by the hardening modulus B, with an effect of 18%, followed then by the thermal softening coefficient m with an effect of 8%. Trends are similar for the thrust force. The increase of parameters B, n, m, and A generates an rising in effort with effects respectively equal to 18 %, 14 %, 8 % and 7 %. Other coefficients and interactions have insignificant effects on these predicted variables. The increase of Johnson-Cook coefficients leads to increase the flow stress. So, the rising in efforts is coherent. The increase of parameters A and C generates an insignificant increase on the cutting forces because at the same time, a decrease of chip thickness and contact length is observed. We note also that the trends due to the in uence of the J-C pa-rameters on the chip characteristics (Fig.7) and the forces (Fig.8) are not the same. In fact, local complex phenomena can explain this remark. For instance, the increase of the chip thickness combined to a severe plastic deformation doesn't generate a proportional increase of the cutting force. At the same time, we note also an increase of the contact length and a reduced increase of the thrust force.

x*y: interaction	**C: strain rate sensitivity coefficient**
A: yield strength	**m: thermal softening coefficient**
B: hardening modulus	**n: hardening coefficient**

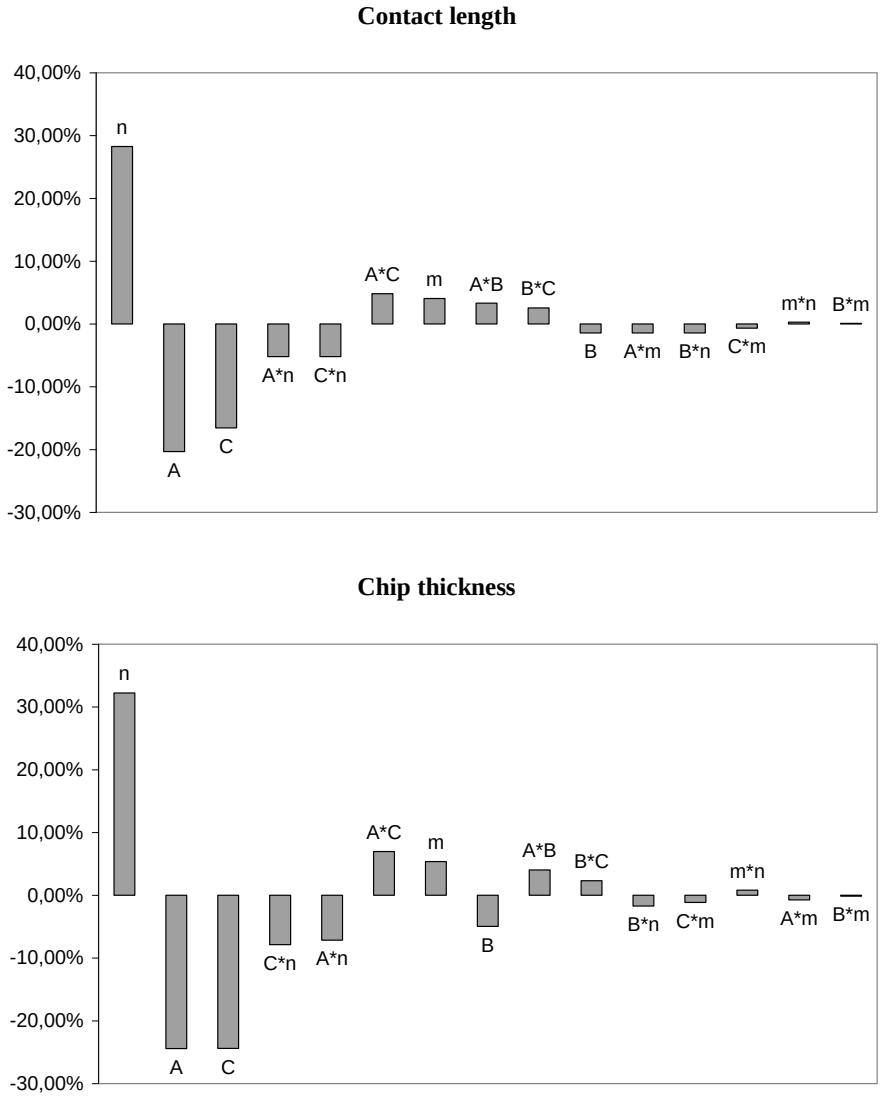

Fig. 7. Impact of Johnson-Cook parameters on the contact length and on the chip thickness.

x*y: interaction	**C: strain rate sensitivity coefficient**
A: yield strength	**m: thermal softening coefficient**
B: hardening modulus	**n: hardening coefficient**

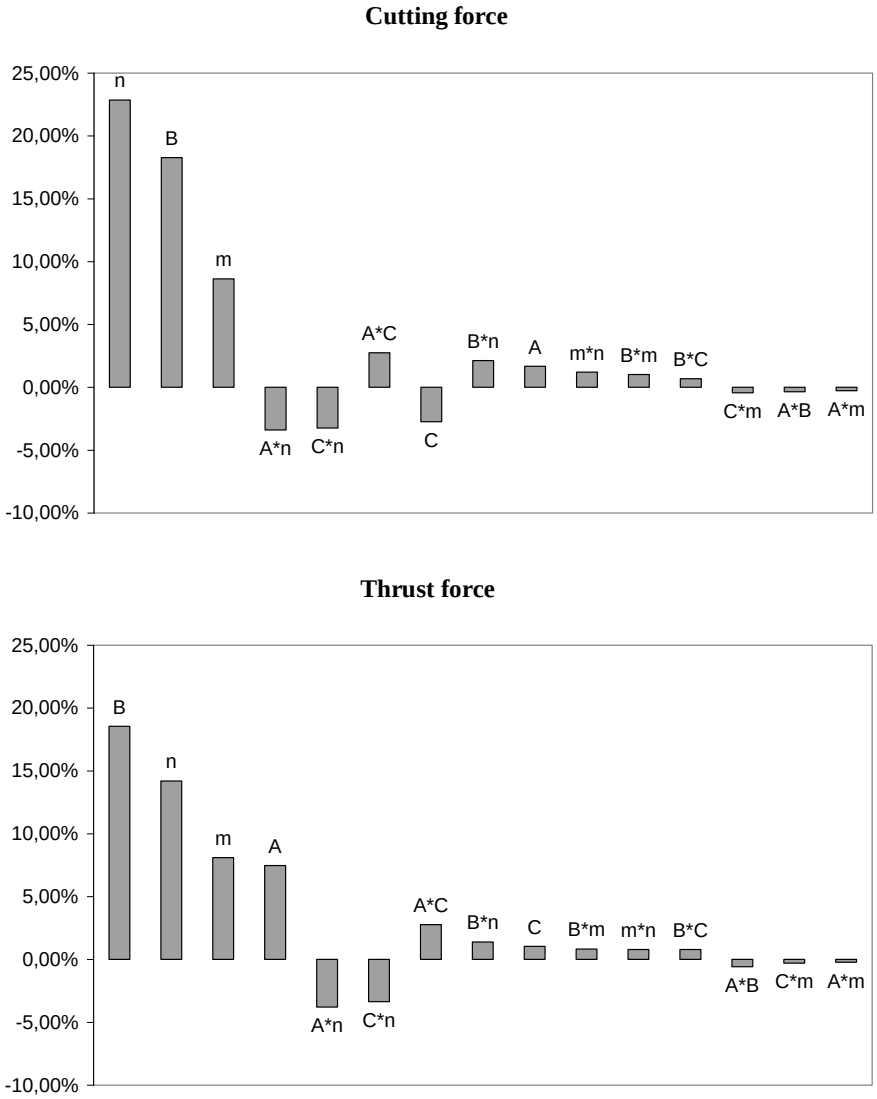

Fig. 8. Impact of Johnson-Cook parameters on the cutting forces.

The presented results are dependent on the variation range. To define the sensitivity of process parameters to the Johnson-Cook coefficients, their impact is assumed to be linear. The tolerance limits of Johnson-Cook coefficients are defined by sensitivities shown in Table 10. The sensitivity of the parameter C is very important. For example by considering parameter C, an increase of unitary value generates an increase of 2143°C on the maximum tool temperature and of 1603°C on the maximum workpiece temperature.

For another example, the numerical prediction of the contact length with an error of 0.025 mm, which corresponds to an error of 5 % for this study, requires the determination of strain rate sensitivity coefficient C with a tolerance limit of 0.006. Table 11 shows tolerance limits necessary to restrict errors on predicted parameters at 5%.

Table 10. Sensitivity of process parameters to the Johnson-Cook coefficients.

	T_o (°C)	T_c (°C)	l_c (mm)	e (mm)	F_c (N)	F_t (N)
A (MPa)	0.218	0.185	-0.000243	-0.000318	0.0586	0.124
B (MPa)	0.344	0.334	-0.000016	-0.000053	0.593	0.285
C	2416	1876	-4.027	-6.472	-1947	351
m	212	212	0.088	0.126	545	243
n	348	401	0.629	0.781	1485	438

Table 11. Required margin identification of Johnson-Cook coefficients.

	ΔT_o=50 °C	ΔT_c=50 °C	Δl_c=25 μm	Δe=15 μm	ΔF_c=40 N	ΔF_t=30 N
***A* (MPa)**	229	270	103	47	683	242
***B* (MPa)**	145	150	1563	283	67	105
C	0.021	0.027	0.006	0.002	0.021	0.085
m	0.236	0.236	0.284	0.119	0.073	0.123
n	0.144	0.125	0.040	0.019	0.027	0.068

3.2. Impact of contact parameters

The main contact parameters are the thermal conductance K, the heat partition coefficient α and the friction coefficient μ. The level values of the contact parameters used for the sensitivity analysis are presented in Table 12. The thermal conductance and heat partition coefficient levels are chosen in accordance works of Pantalé (1996) and Briot et al. (1997). The values of the friction coefficients are in the range 0.3-0.6. This is in accordance with the three frictional regimes recently described by Ben Abdelali et al. (2011).

Table 12. Level values for contact parameters.

	Low level	**High level**
Thermal conductance *K* ($W.m^{-2}.°C^{-1}$)	10^3	10^8
Heat partition coefficient α	0.25	0.75
Friction coefficient μ	0.3	0.6

The change of heat partition coefficient α from law level to high level generates a decrease of the maximum tool temperature of about 40 % and a decrease of the maximum workpiece temperature of 5 % as shown in Fig. 9. The friction coefficient has a predominant impact in the increase of the maximum tool temperature, with an effect of 15 %.

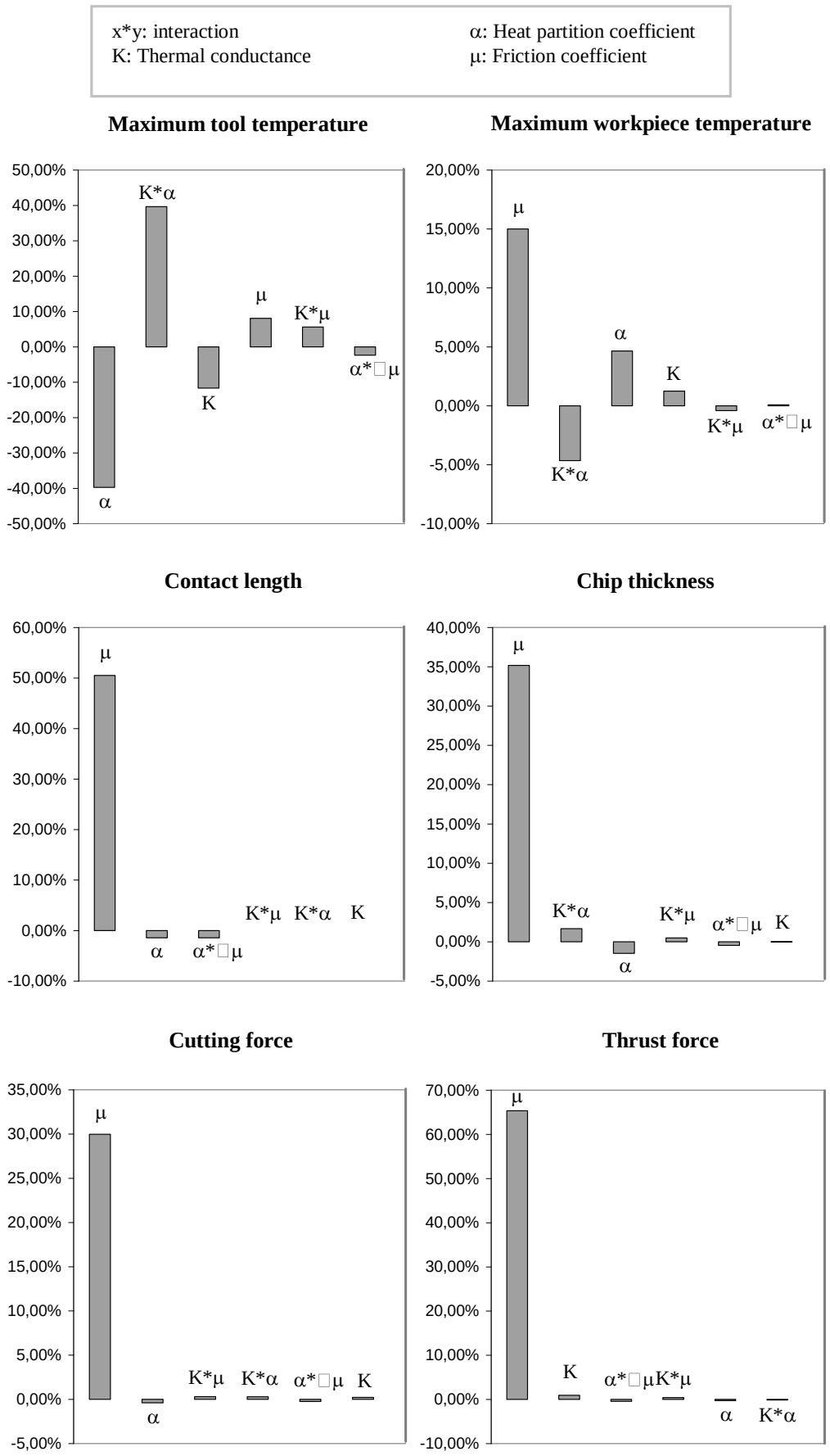

Fig. 9. Impact of contact parameters on the process variables.

The maximum tool temperature is strongly affected by the interaction between heat partition coefficient α and thermal conductance K. The thermal conductance effect is increased (28 % compared to -12 %) when heat partition coefficient α is equal to 0.75. The coefficient α has no impact when thermal conductance K is equal to 10^8 $W.m^{-2}.°C^{-1}$. This remark remains valid for the maximum tool temperature. So, in the case of perfect thermal contact, the temperature at the tool-chip interface is not affected by the heat transfer partition coefficient α. As far as other process variables are concerned, only the friction coefficient has a significant effect. Increases of 65 %, 50%, 35 %, and 30 % are respectively observed on thrust force, contact length, chip thickness and cutting force.

The impact of the contact parameters is also assumed to be linear and the sensitivities of process variables to contact parameters are given in Table 13. In order to simulate process variables with a maximum error of 5 %, the contact parameters should be identified with tolerance limits given by Table 14. Thus, thermal conductance K and heat partition coefficient α can be identified without good accuracy, while friction coefficient μ has to be determined with a tolerance limit of less than 0.03. However, an accurate identification of the heat partition coefficient (tolerance limits of 0.064) is needed to get a good prediction of the maximum tool temperature.

Table 13. Sensitivity of process parameters to the contact parameters.

	T_o	T_c	l_c	e	F_c	F_t
K	$-1.15\ 10^{-6}$	$1.14\ 10^{-7}$	0	$-4.00\ 10^{-13}$	$2.08\ 10^{-8}$	$4.70\ 10^{-8}$
α	-783	86	-0.010	-0.010	-7.512	-2.575
μ	264	461	0.591	0.410	945	1096

Table 14. Required margin identification of contact parameters.

	ΔT_o=50°C	ΔT_c=50°C	Δl_c=25 µm	Δe=15 µm	ΔF_c=40 N	ΔF_t=30 N
K	$4{,}35\ 10^{7}$	$4.39\ 10^{8}$	_	$3.75\ 10^{10}$	$1.92\ 10^{9}$	$6.38\ 10^{8}$
α	0.064	0.581	2.500	1.500	5.325	11.650
μ	0.189	0.108	0.042	0.037	0.042	0.027

3.3. Impact of thermal parameters

The impact of workpiece and tool conductivities and their specific heats are studied with a two-level factorial design. Level values are shown in Table 15.

Table 15. Level values for thermal parameters.

	Minimum value	Maximum value
k_p	24.9	45.1
k_o	25	80
c_p	435.3	1171
c_o	200	480

The workpiece specific heat c_p and the tool conductivity k_o are the only factors which have a significant impact on maximum temperature at tool-chip interface as reported fig. 10. The increase of the workpiece specific heat generates a decrease of maximum temperature at tool-chip interface (25%). When the tool conductivity increases, the maximum tool temperature decreases of 15 % as against 10 % for the maximum workpiece temperature.

Fig. 10. Impact of thermal parameters on the maximum temperatures.

Only workpiece specific heat has a significant impact on other process parameters as shown in Figs. 11-12. The increase of the workpiece specific heat generates an increase of process parameters (from 25 % to 35 %).

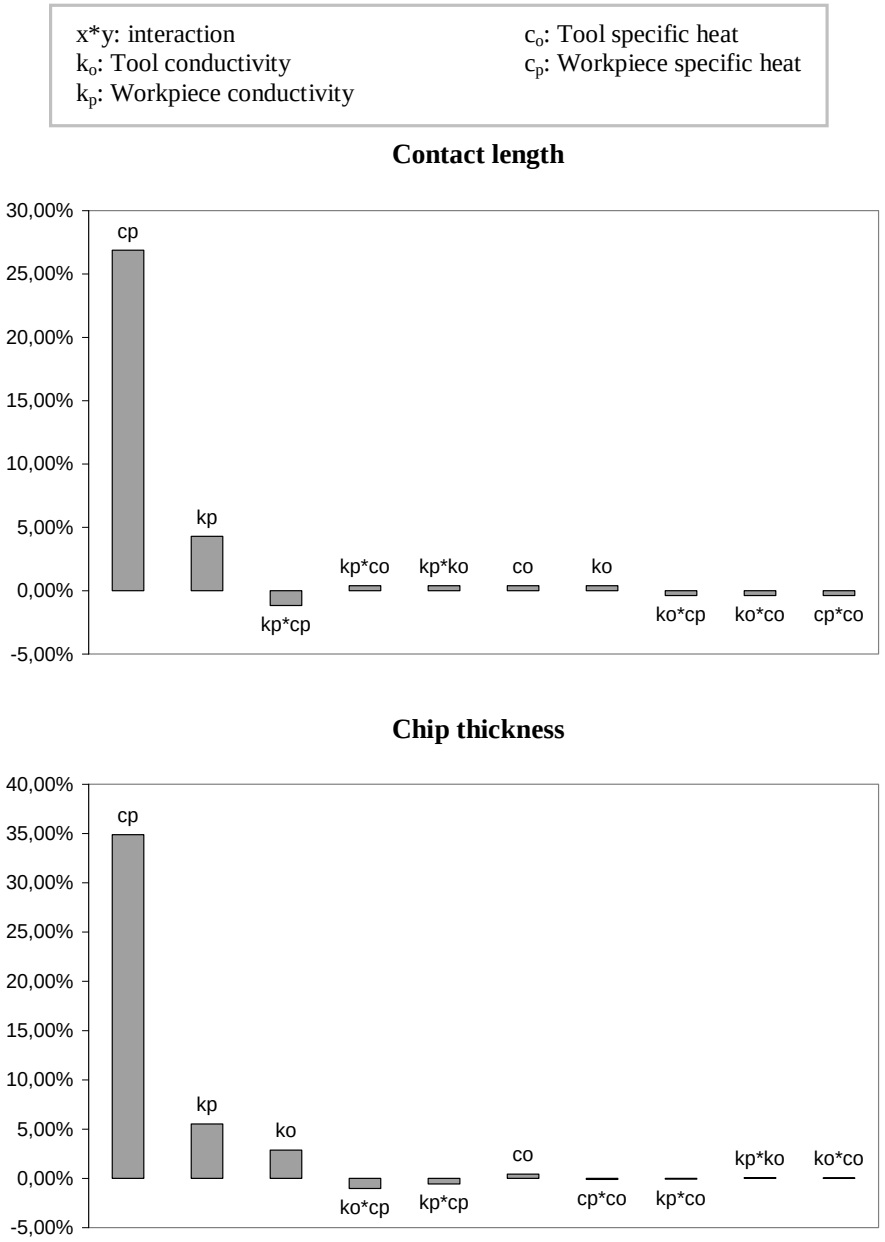

Fig. 11. Impact of thermal parameters on the contact length and on the chip thickness.

x*y: interaction
k_o: Tool conductivity
k_p: Workpiece conductivity
c_o: Tool specific heat
c_p: Workpiece specific heat

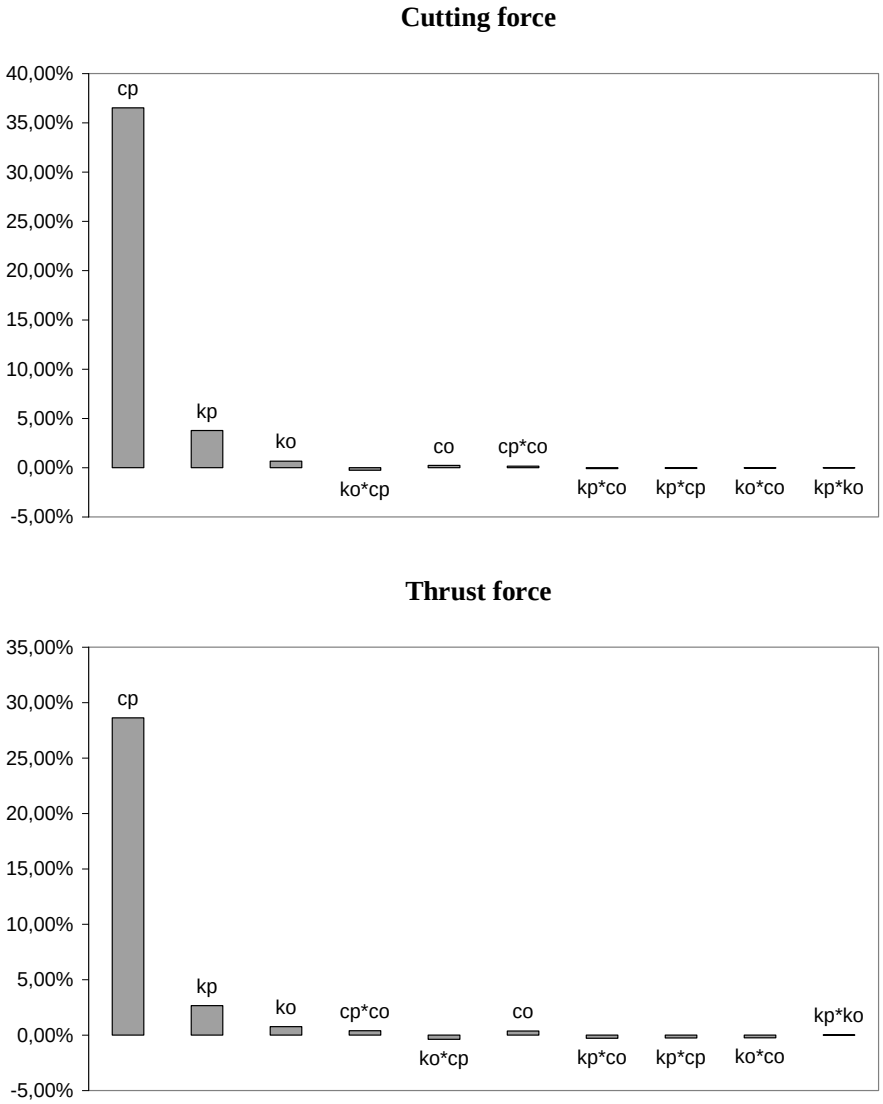

Fig. 12. Impact of thermal parameters on the cutting forces.

The sensitivities of the process variables to the thermal parameters are defined with the assumption of linear variations given by Table 16.

Table 16. Sensitivity of process parameters to the thermal parameters.

	T_o	T_c	l_c	e	F_c	F_t
k_p	-1.800	-2.192	0.000689	0.000960	1.854	0.618
k_o	-2.435	-1.440	0.000023	0.000183	0.119	0.066
c_p	-0.234	-0.285	0.000119	0.000166	0.493	0.183
c_o	-0.064	-0.040	0.000005	0.000005	0.008	0.006

The tool conductivity and the tool specific heat (respectively k_o et c_o) have an insignificant impact. So, thermal parameters of tool can be determined with large tolerance limits reported in Table 17. Workpiece thermal parameters are on the contrary more significant. For example, the workpiece conductivity should be identified with a tolerance limit of around 30 $W.m^{-1}.°C^{-1}$ to simulate the process variables with a maximum error of 5 %.

Table 17. Tolerance limits of thermal parameters.

	ΔT_o=50 °C	ΔT_c=50 °C	Δl_c=25 µm	Δe=15 µm	ΔF_c=40 N	ΔF_t=30 N
k_p	28	23	36	16	22	49
k_o	21	35	1086	82	336	458
c_p	214	175	211	90	81	164
c_o	776	1244	5528	2781	4959	4821

Temperature-dependent parameters are the aim of the second sensitivity study. Only the workpiece parameters (i.e. k_p and c_p) are considered. The low and high levels are defined respectively adding and subtracting 5 % to the reference values as shown in Fig. 12.

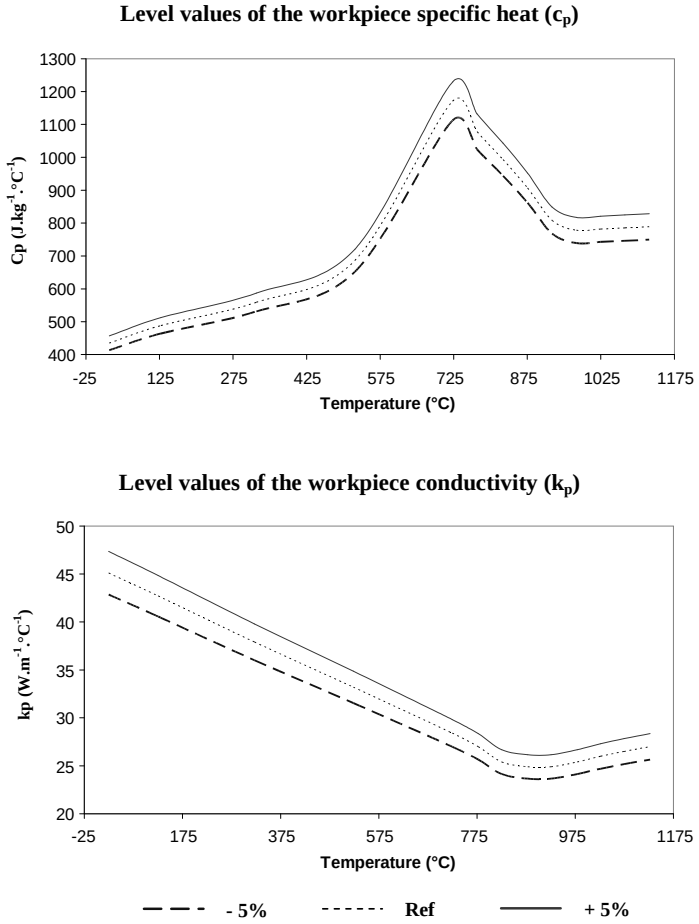

Fig. 13. Level values for temperature-dependant parameters of the workpiece.

This study shows that a tolerance limit of +/- 5 % on conductivity and specific heat is enough to simulate the process variables with an error less than 5 % as illustrated in Fig. 14. These results, firstly unexpected, underline the greater extent of rheological and contact parameters than the thermal properties of the tool and workpiece materials.

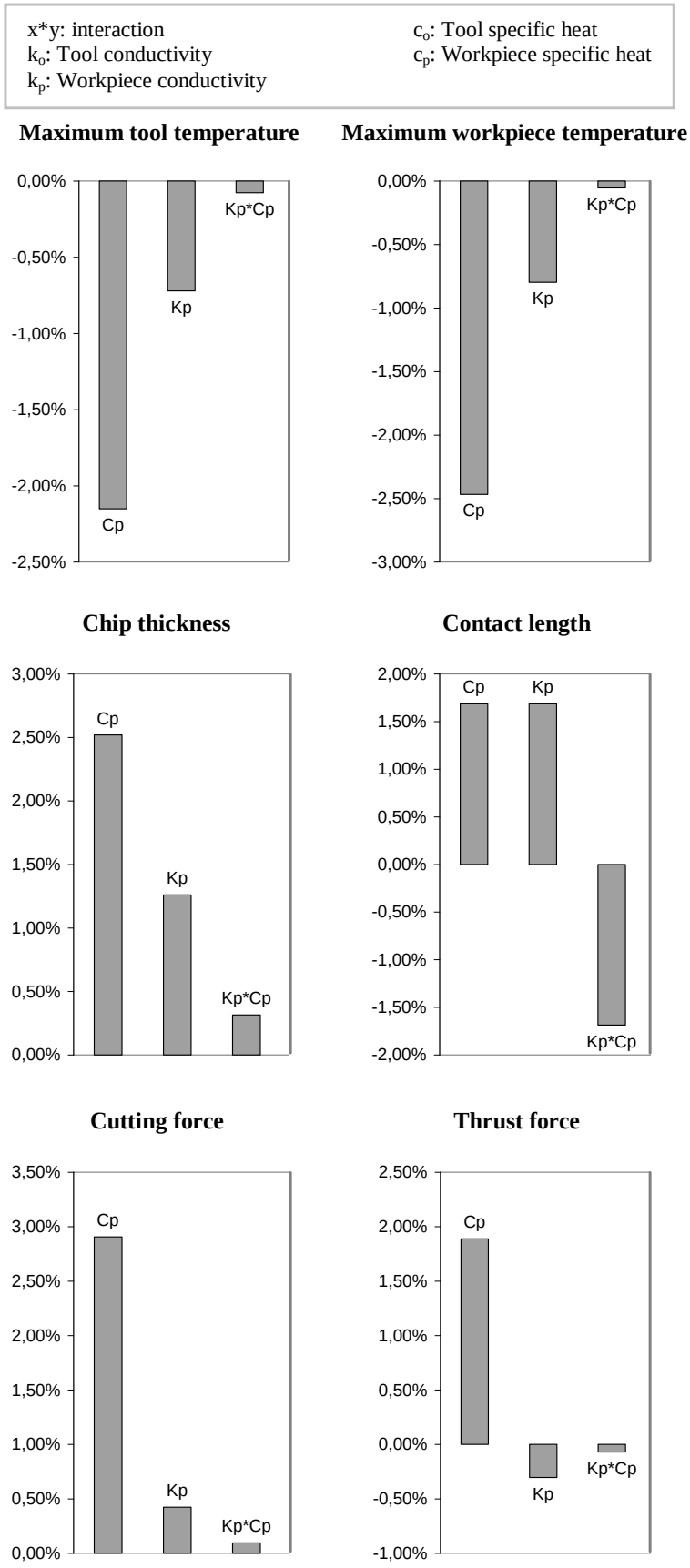

Fig. 14. Impact of workpiece thermal parameters on the process variables.

4. Conclusions

A two-dimensional finite element model of orthogonal cutting with an ALE formulation has been developed with a commercial software code ABAQUS. The initial chip geometry must be define near enough to the expected final chip shape in order to limit the numerical instability. Significant errors on the trust force and on the contact length are highlighted compared with the experimental values obtained by Filice et al. (2006) during an orthogonal cutting test of an AISI 1045 steel with an uncoated carbide. The numerical model of orthogonal cutting is then used to study the sensitivity of process parameters to input parameters.

The sensitivity analysis has allowed the identification of significant input parameters and the determination of their tolerance limits. First, the rheological constants of the Johnson-Cook's law are tested. The sensitivity strain rate coefficient C has the most significant impact and it must be identified with a tolerance limit of 0.006. The tolerance limits of thermal softening coefficient m and hardening coefficient n are also restricted (from 0.02 to 0.3). On the contrary, the process variables are not affected by the yield strength A and the hardening modulus B.

A second study carried out with contact parameters shows that the friction coefficient has a main impact on the process variables. The identification of this coefficient with a tolerance limit of around 0.03 is needed to simulate the process variables with an error less than 5 %. The maximum temperature at the tool-chip interface is affected by the thermal conductance K and by the heat partition coefficient α. A considerable interaction between these both parameters is observed and a special attention is needed to their identification.

In a third part, the effect of the thermal parameters (conductivity and specific heat) to process variables has been studied. The tool parameters have an insignificant impact, while workpiece conductivity and workpiece specific heat are more significant. However, the identification of these parameters as a function of temperature allows to simulate the process variables with errors less than 5 %.

This study draws to input parameters which have to be determine accurately as far as possible in order to improve numerical approaches of machining.

5. Acknowledgments

The authors are grateful to the foundation de France / CETIM for supporting this work. The present research work has been supported by International Campus on Safety and Intermodality in Transportation the Nord-Pas-de-Calais Region, the European Community, the Regional Delegation for Research and Technology, the Ministry of Higher Education and Research, and the National Center for Scientific Research. The authors gratefully acknowledge the support of these institutions.

References

Ben Abdelali H., . Claudin C, Rech J., Ben Salem W., Kapsa Ph., Dogui A., 2011. Experimental characterization of friction coefficient at the tool–chip–workpiece interface during dry cutting of AISI 1045, Wear, In press, Corrected Proof

Bonnet C., Valiorgue F., Rech J., Claudin C., Hamdi H., Bergheau J.M., Gilles P., 2008. Identification of a friction model – Application to the context of dry cutting of an AISI 316L austenitic stainless steel with a TiN coated carbide tool, International Journal of Machine Tools and Manufacture 48, 1211-1223.

Briot J-M., Bourouga B., Bardon J-P., 1997. Étude de la conductance thermique de transport entre les bagues d'un roulement à rouleaux, Revue Générale de Thermique 36, 610-623.

Brocail J., Watremez M., Dubar L., 2010. Identification of a friction model for modelling of orthogonal cutting, International Journal of Machine Tools and Manufacture 50, 807-814.

Brocail J., Watremez M., Dubar L., Bourouga B., 2008. Contact and friction analysis at tool-chip interface to high-speed machining, International Journal of Material Forming 1, 1407-1410.

Filice L., Micari F., Rizzuti S., Umbrello D., 2006. A critical analysis on the friction modelling in orthogonal machining, International Journal of Machine Tools and Manufacture 47, 709-714.

Grzesik W., Nieslony P., 2004. Prediction of friction and heat flow in machining incorporating thermophysical properties of the coating-chip interface, Wear 256, 108-117.

Haglund A.J., Kishawy H.A., Rogers R.J., 2008. An exploration of friction models for the chip-tool interface using an Arbitrary Lagrangian-Eulerian finite element model, Wear 265, 452-460.

Jaspers S.P.F.C., Dautzenberg J.H., 2002. Material behaviour in conditions similar to metal cutting: flow stress in the primary shear zone, Journal of Materials Processing Technology 122, 322-330.

Jovic C., Wagner D., Herve P., Gary G., Lazzarotto L., 2006. Mechanical behaviour and temperature measurement during dynamic deformation on split Hopkinson bar of 304L stainless and 5754 aluminium alloy, Journal of Physic IV 134, 1279-1285.

Kalhori V., 2001. Modeling and simulation of mechanical cutting, Phd Thesis, Université de Lunea Tekniska.

Meyer L.W., Halle T., Herzig N., Krüger L., Razorenov S.V., 2006. Experimental investigations and modelling of strain rate and temperature effects on the flow behaviour of 1045 steel, Journal de Physique IV France 134, 75–80.

Meiller M., Lebrun J.L., Touratier M., Ryckelynck D., 2000. Friction law for tool-workpiece contact area in dry machining, International Workshop on Friction and Flow Stress in Cutting and Forming, France, 101-109.

Outeiro J.C, Dias A.M., Lebrun J.L., 2004. Experimental assessment of temperature distribution in three dimensional cutting process, Machining Science and Technology 8, 357-376.

Olsson M., Söderberg S., Jacobson S., Hogmark S., 1989. Simulation of cutting tool wear by a modified pin-on-disc test, International Journal of Machine Tools and Manufacture 29, 377-390.

Özel T., 2006. The influence of friction models on finite element simulations of machining, International Journal of Machine Tools and Manufacture 46, 518-530.

Özel T., Altan T., 2000. Determination of workpiece flow stress and friction at the chip–tool contact for high-speed cutting, International Journal of Machine Tools and Manufacture 40, 133-152.

Özel T., Karpat Y., 2007. Identification of constitutive material model parameters for high-strain rate metal cutting conditions using evolutionary computational algorithms, Materials and Manufacturing Processes 22, 659-667.

Pantalé O., 1996. Modélisation et simulation tridimensionnelles de la coupe de métaux, Phd Thesis, Université de Bordeaux I.

Rech J., Claudin C., D'Eramo E., 2009. Identification of a friction model - Application to the context of dry cutting of an AISI 1045 annealed steel with a TiN-coated carbide tool, Tribology International 42, 738-744

Rosakis P., Rosakis A.J., Ravichandran G., Hodowany J., 2000. A thermodynamic internal variable model for the partition of plastic work into heat and stored energy metals, Journal of the Mechanics and the Physics of Solids 15, 581-607.

Umbrello D., M'Saoubi R., Outeiro J.C., 2007. The influence of Johnson-Cook material constants on finite element simulation of machining of AISI 316L steel, International Journal of Machine Tools and Manufacture 47, 462-470.

Yen Y.-C., Jain A., Altan T., 2004, A finite element analysis of orthogonal machining using different tool edge geometries, Journal of Materials Processing Technology 146, 72-81.

List of figures :

List of tables :